

Equation of State Data and Electrical Resistivity Of Hot Expanded Al-Au Mixture

P. Renaudin, J. Clérouin, P. Noiret, V. Recoules

Département de Physique Théorique et Appliquée

CEA/DAM Ile-de-France, BP12, 91680 Bruyères-le-Châtel Cedex, France

There has been a growing interest in the exploration of atomic properties of strongly coupled partially degenerate plasmas, also referred to warm dense matter (WDM). This thermodynamic regime is encountered in the structural formation of hydrogen-bearing astrophysical objects [1], Jovian planets' interior [2], extrasolar giant planets [3], brown dwarfs [4] and low mass stars [5]. One of the most important problems emerging from the astrophysical literature is the need of accurate equation of state (EOS) in the regime of WDM.

Studies of WDM is a challenging field of research for both experiments and theoretical calculations. From the experimental point of view, WDM's equation of state have been first studied by investigated shocked states which are easier to generate, diagnose and analyze than unshocked states. The majority of dynamic EOS data has been measured along the principal Hugoniot, leaving a scarcity of data in regimes off the Hugoniot, such as hot expanded matter.

In this paper, we report on the combined electrical resistivity, pressure, and internal energy variation measurements of a gold-aluminum mixture plasma. The experiments were performed in an isochoric plasma closed-vessel (EPI) where a sample goes from the solid-state at normal density and room temperature to a well-known density plasma regime in the internal energy range 8-12 MJ/kg. The goal of this paper is to show that quantum molecular dynamics simulations are particularly well suited for describing this regime and are providing a consistent view of the system in terms of the EOS and the transport properties, even for a mixture plasma which present a complex electronic structure.

The experiments were performed in EPI, which has been described in details in previous papers [6]. EPI combines two techniques: a high-pulse power-bank to obtain a fast heating of the metallic sample and a high-pressure closed-vessel build in sapphire that mechanically controls the plasma volume. The sapphire rings are bound in the middle of high-pressure tungsten carbide rings forming (one stacked) a tube of 19 cm in length and 1.2 cm in diameter. This facility allows an absolute measurements of the internal energy, pressure and

electrical resistance. The amount of matter in the chamber yields the exact density of the homogeneous plasma phase. Current is driven from four capacitors connected in parallel, totalling 2.42 mF, and is switched by a pressurized spark gap switch. Internal inductance of the circuit is 6 μ H. With such setup, the sample is heated in a hundred of microseconds. A Rogowski belt surrounds one electrode to measure the time derivative of the current and a resistive divider is used to measure the voltage drop across the plasma. The time derivative dI/dt of the current and the inductance L of the plasma are small enough to make the $L \times dI/dt$ term negligible compared to the measured voltage, except at the very beginning of the discharge. Therefore, no inductive correction is needed to obtain the plasma resistivity from the current and voltage measurements. Two piezoelectrical sensors with 2- μ s rise time are placed at each end of the vessel to measure the pressure during the discharge. Note that all quantities are known versus the internal energy variation. To preserve the quality of our data we will show them this way. The uncertainties in the measurements of the conductivity and the internal energy variation are related to the accuracy of current and voltage measurements and are estimated at about 15%.

Quantum molecular dynamics (QMD) has been used to calculate the thermodynamic and optical properties of the studied plasma. In QMD, the ions follow classical trajectories determined by the forces acting on them while the electronic subsystem remains in ground state at each instant. The equations of motions for the ions are solved via the velocity Verlet algorithm. The forces are calculated from the electronic ground state using the Hellman-Feynman theorem. For each positions of the ions, the ground state electronic density is computed by minimizing the free energy functional of the electron gas in the framework of finite temperature density functional theory. In this work, the exchange and correlation term in the density functional expression is represented by the local density approximation. It is expressed from the exchange and correlation energy of a uniform electrons gas with the same electronic density as the one of the system. We used the energy estimation computed by Ceperley and Adler using a Monte-Carlo method [7]. The projector augmented wave method is used to construct electron-ion potential [8]. Only valence electrons are explicitly represented. The Au $5d$ and $6s$ electrons and Al $3s$ and $3p$ electrons are counted as valence electrons, and all more tightly bond electrons are counted as part of the core. QMD simulations for warm dense Au_xAl_{1-x} with x equal to 0., 0.03, 0.19, 0.37, 0.62, and 1. were performed for four temperatures ranging from 15000 K to 30000 K. A cubic cell of size appropriate to reproduce the experimental density is used with periodic boundary

conditions of the simple cubic type. Electronic orbital are populated according to the Fermi-Dirac distribution function with a number of states lying from 1000 to 1500. Trajectories are generated in the microcanonical ensemble for 500 time steps of 2 fs. In this ensemble, the system remains free to adjust to an average equilibrium ionic temperature, and the total energy should be conserved. For all simulations, we use the VASP plane-wave code [9]. In linear response theory, the real part of the frequency dependent conductivity is given in terms of Kubo-Greenwood equation [10]. A QMD simulation of the solid phase at 300 K sets the reference energy. All further energies are given relative to this reference energy, allowing a direct comparison between theoretical results and experimental data.

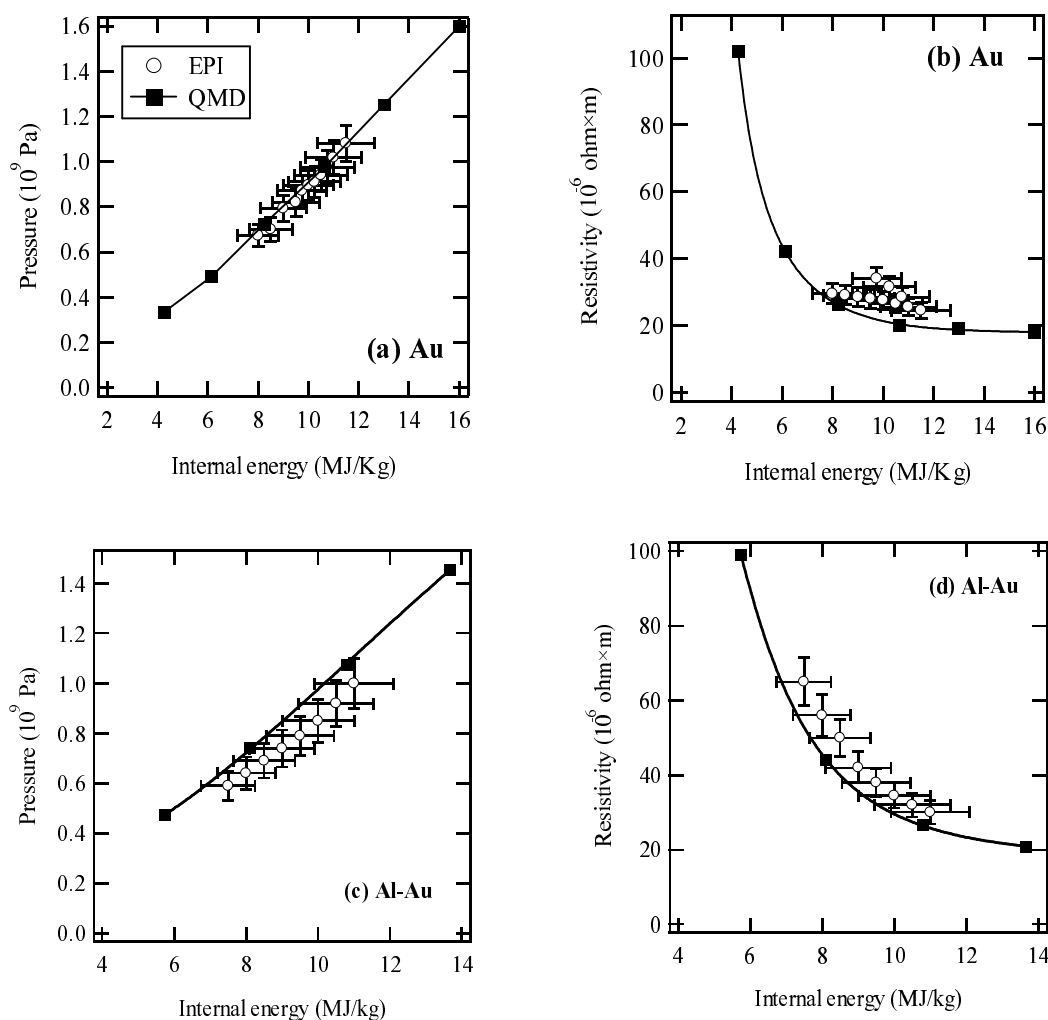


Figure 1: Experimental data and theoretical calculations versus internal energy variation for Au at 0.5 g/cm^3 and $\text{Au}_{0.62}\text{Al}_{0.38}$ at a density of 0.5 g/cm^3 .

The experimental data and QMD calculations are reported in Fig. 1a and Fig. 1b in the case of pure gold plasma at a density of 0.5 g/cm^3 . The experimental data and QMD calculations are reported in Fig. 1c and Fig. 1d in the case of $\text{Au}_{0.62}\text{Al}_{0.38}$ plasma at a density of 0.51 g/cm^3 . The QMD pressures agree perfectly with experimental results. This excellent agreement demonstrates that the QMD describes very accurately the fluid and also the various density effects in the thermodynamic regime of the experiment. In various atomic models, density effects such as pressure ionization and plasma ion correlation are entered through the ion sphere model or in a more phenomenological way, in contrast with QMD calculations [11]. The QMD electrical resistivities agree well with the experimental data. This good agreement shows that the Kubo-Greenwood formulation of the electrical conductivity is accurate for the warm dense mixture.

To conclude we have performed the first measurement of equation of state data and electrical resistivity of warm dense plasma and fluid gold and aluminum mixture. QMD calculations are in good agreement with the experimental data in the internal energy range 8-12 MJ/kg. Therefore, in this thermodynamic regime, QMD can be used to test (1) the accuracy of some mixing rule models, such as partial density mixing rule or isothermal-isobaric mixing rule and (2) the accuracy of the theoretical models used to modelized the dynamical properties of giant planets [12].

References

- [1] H.M. Van Horn, *Science* **252**, 384 (1991).
- [2] W.J. Nellis, M. Ross and N.C. Holmes, *Science* **269**, 1249 (1995).
- [3] T. Guillot, *Science* **286**, 72 (1999).
- [4] A. Burrows and J. Liebert, *Rev. Mod. Phys.* **65**, 301 (1993).
- [5] G. Chabrier and I. Barafe, *Astron. Astrophys.* **327**, 1039 (1997).
- [6] P. Renaudin *et al.*, *Phys. Rev. Lett.* **88**, 215001 (2002); **91**, 075002 (2003).
- [7] D. M. Ceperley and B. J. Alder, *Phys. Rev. Lett.* **45**, 566 (1980).
- [8] G. Kresse and D. Joubert, *Phys. Rev. B* **59**, 1758 (1999).
- [9] G. Kresse and J. Hafner, *Phys. Rev. B* **47**, R558 (1993); G. Kresse and J. Furthmuller, *Comput. Mater. Sci.* **6**, 15 (1996).
- [10] V. Recoules *et al.*, *Phys. Rev. E* **66**, 56412 (2002).
- [11] P. Renaudin *et al.*, *Phys. Rev. E* **73**, 56403 (2006).
- [12] D. Saumon and T. Guillot, *Astrophysical Journal* **609**, 1170 (2004).